The final version of this manuscript has appeared in IEEE Wireless Communications Letters, vol.3, no.1, pp.10,13, February 2014
Available online: http://ieeexplore.ieee.org/xpl/articleDetails.jsp?arnumber=6648515
DOI: 10.1109/WCL.2013.100913.130631

RSS-based ranging by multichannel RSS averaging

Andrea Zanella and Andrea Bardella
Department of Information Engineering
University of Padova, Padova, Italy
Emails: {zanella, bardella}@dei.unipd.it
May 13, 2014

***Abstract*—This letter shows that the accuracy of Radio Signal Strength (RSS)-based ranging can be increased by averaging RSS samples collected on different RF channels. Starting from a multi-cluster propagation model, the analysis shows that Multi Channel RSS Average (MCRA) can indeed reduce the component of the RSS variability due to self-interference produced by strong and quasi-static multipath replicas of the received signal, while it is ineffective against fading components caused by obstacles blockage. The theory is backed up by a set of experimental results obtained in different scenarios that confirm the capability of MCRA to effectively reduce RSS variability and increase RSS-based ranging accuracy.**

I. Introduction

The suitability of Received Signal Strength (RSS) for ranging in wireless networks has been long debated by the scientific community. The approach is attractive because RSS indication is made readily available by all common wireless transceivers but, on the other hand, RSS measurements are often unreliable and may yield large ranging errors [1]–[5]. While time variability can be attenuated by averaging out the RSS samples over time, space-dependent variability cannot be easily reduced when nodes are static and equipped with single antenna.

In this letter, we propose multichannel RSS average (MCRA) as a simple means to reduce the variability of RSS measurements and, in turn, increase the accuracy of RSS ranging. Despite its simplicity, the exploitation of multichannel diversity to enhance RSS ranging has not received much attention by the scientific community. This is probably due to the misconception about the nature of the space-dependent variability of RSS measurements, which is commonly ascribed to the shadowing phenomenon, i.e., the attenuation of the signal strength due to obstacles along the path to the receiver. In this case, indeed, the spatial diversity provided by a few MHz shift of the carrier frequency would not be sufficient to counteract the spatial correlation of the shadowing. In practical settings, however, the space–dependent RSS variability is often due to *self-interference* among *strong* multipath signal components that overlap at the receiver with random phases [6]–[8]. In this letter we show that MCRA is effective against *this* component of the space-dependent RSS variability, while it is actually unavailing when shadowing is *only* caused by obstacle blockage.

Channel diversity has been recently considered in [9] to estimate the parameters of a simplified ray-tracing signal propagation model, which allows for anchor-free node localization. While less powerful and sophisticated than [9], yet the MCRA method proposed in this letter is interesting because of its extreme simplicity and effectiveness in reducing the variability of RSS measurements and enhancing RSS-based ranging accuracy.

The rest of the letter is organized as follows. Sec. II describes the prevalent RSS ranging model based on the *pathloss plus shadowing* propagation model. Sec. III investigates the impact of MCRA on RSS variability by using a simple multi-cluster propagation model [7], [8]. The theoretical argumentation is backed up in Sec. IV by a series of experimental results obtained in different scenarios. Sec. V finally concludes the letter by summarizing the main achievements.

II. RSS ranging

Let $\mathbf{s}$ denote the positions of a pair of transceivers, and let $d = \|\mathbf{s}\|_2$ be the line-of-sight (LOS) geographical distance between the two nodes. The RSS measured at time t by the receiver can be expressed (in dB scale) as

$$\rho(t, \mathbf{s}) = D(d) + E(t, \mathbf{s}) \tag{1}$$

where $D(d)$ accounts for the deterministic part of the power-decay law, and $E(t, \mathbf{s})$ is a random variable that accounts for all random factors that affect the received signal power.

A common model for $D(d)$ is the *one-slope path loss propagation model* [6], according to which

$$D(d) = \mathcal{K} - 10\eta \log(d/\delta_0) \tag{2}$$

where δ_0 is the distance after which the far-field assumption holds and the path loss model is valid, whereas $\mathcal{K}$ collects all the other constant factors that may affect the received power.

The noise term $E(t, \mathbf{s})$ is normally modeled as a combination of *short-term* and *long-term* fading. The first accounts for the time variability of the received signal due to quick random changes of the propagation conditions [10], [11]. The long-term fading is often referred to as *shadowing* and typically modeled as a lognormal random variable in linear scale, which becomes a normal random variable in dB scale [6], [11]. The shadowing is assumed position-dependent, but almost time invariant.

Therefore, averaging out RSS samples collected in different time instants, as typically done before performing RSS-based ranging, one reduces the impact the short-term fading components of RSS, but leaves basically unaltered the long-term fading. Accordingly, the time-averaged RSS can be expressed as

$$\bar{\rho}(\mathbf{s}) = \mathcal{K} - 10\eta \log(d/\delta_0) + \Psi^{\mathrm{dB}} \tag{3}$$

where $\Psi^{\mathrm{dB}} = 10\log(\Psi)$ represents the long-term fading (shadowing) that, *in dB scale*, is commonly modeled as a zero-mean normal random variable with standard deviation $\sigma_{\Psi^{\mathrm{dB}}}$ that ranges from 2 to 6 in indoor environments [6]. The parameters δ_0, $\mathcal{K}$, η, and $\sigma_{\Psi^{\mathrm{dB}}}$ depend on the environment and can be estimated from local measurements, for instance using the classical Least-Square (LS) method [6].

Given the (time-averaged) RSS value r, the Maximum Likelihood Estimate (MLE) of the transmitter-receiver distance is given by

$$\hat{d}(r) = \delta_0 10^{\frac{\mathcal{K}-r}{10\eta}} \ . \tag{4}$$

Replacing r with the random variable $\bar{\rho}(\mathbf{s})$, we get

$$\hat{d} = d\, 10^{-\frac{\Psi^{\mathrm{dB}}}{10\eta}} = d\, \Psi^{-1/\eta} \tag{5}$$

where $\Psi = 10^{\Psi^{\mathrm{dB}}/10}$ is lognormal distributed, with parameters $\mu = 0$ and $\sigma = \sigma_{\Psi^{\mathrm{dB}}}/A$, with $A = 10\log(e)$.

The *normalized ranging error* can then be defined as

$$\varepsilon_r = \frac{d-\hat{d}}{d} = 1 - \Psi^{-1/\eta} \tag{6}$$

whose mean and variance are equal to

$$\mathrm{m}_{\varepsilon_r} = 1 - e^{\frac{\sigma^2}{2\eta^2}} \ ; \quad \sigma^2_{\varepsilon_r} = e^{\frac{2\sigma^2}{\eta^2}} - e^{\frac{\sigma^2}{\eta^2}} \ . \tag{7}$$

From (7) we see that both mean and variance of the ranging error can be reduced by minimizing σ, i.e., $\sigma_{\Psi^{\mathrm{dB}}}$. In the following section we show that MCRA can significantly reduce $\sigma_{\Psi^{\mathrm{dB}}}$, depending on the characteristics of the environment and the frequency band that can be used for multichannel RSS harvesting.

III. Theoretical analysis

According to the multipath propagation model, the signal propagates isotropically from the transmitting antenna and gets scattered by floor, ceiling, walls, and objects, thus reaching the receiver in a number of *multipath components* that may have relatively large delay spread. Each component may result from a single reflector or multiple reflectors clustered together that generate multiple waves with strongly correlated powers and similar delays [7], [8].

Suppose that the transmitted signal arrives to the receiver in N multipath components, each consisting in a cluster of waves. Let α_n, τ_n, and θ_n denote the amplitude, delay and phase rotation, respectively, associated to the nth component, with $n = 1, \ldots, N$. Although small variations of the environment in close proximity to the receiver, due to moving people or machineries, may yield rapid variations of the amplitude α_n, the waves clustering remains almost the same, so that the mean group delay τ_n and phase rotation θ_n can be assumed time invariant. Instead, all parameters clearly depend on the transceivers position, though we omit the $\mathbf{s}$ argument for notation convenience.

For narrowband channels, the equivalent lowpass channel impulse response can then be expressed as

$$h(t,\mathbf{s}) = \sum_{n=1}^{N} \alpha_n e^{-j(2\pi f_c \tau_n - \theta_n)} \tag{8}$$

where f_c is the carrier frequency. Thus, the channel gain is

$$\gamma(t,\mathbf{s}) = |h(t,\mathbf{s})|^2 = \sum_{n=1}^{N} \alpha_n^2 + \sum_{n=1}^{N} \sum_{\substack{m=1 \\ m\neq n}}^{N} \alpha_n \alpha_m \cos\left(\phi_{n,m}\right) \ , \tag{9}$$

where, for brevity, we set

$$\phi_{n,m} = 2\pi f_c \tau_{n,m} + \theta_{n,m} \ , \ \tau_{n,m} = \tau_n - \tau_m \ , \ \theta_{n,m} = \theta_m - \theta_n \ . \tag{10}$$

The random process $\gamma(t,\mathbf{s})$ is an alternative representation of the RSS measured by nodes in position $\mathbf{s}$, expressed in linear scale. Therefore, the variance of the RSS is proportional to the variance of $\gamma(t,\mathbf{s})$. In the following we analyze the effect of time and multichannel averages on $\gamma(t,\mathbf{s})$ and its variance.

Time averaging yields

$$\bar{\gamma}(\mathbf{s}) = \lim_{T\to\infty} \int_0^T \gamma(t,\mathbf{s}) dt = \sum_{n=1}^{N} \overline{\alpha_n^2} + \sum_{\substack{n,m=1 \\ m\neq n}}^{N} \overline{\alpha}_n \overline{\alpha}_m \cos\left(\phi_{n,m}\right) \tag{11}$$

where $\overline{\alpha}_n$ and $\overline{\alpha_n^2}$ denote the time average of α_n and α_n^2, respectively. Performing MCRA over C RF channels spaced apart by a bandwidth B_c we get

$$\bar{\bar{\gamma}}(\mathbf{s}) = \frac{1}{C} \sum_{h=0}^{C-1} \left[\sum_{n=1}^{N} \overline{\alpha_n^2} + \sum_{\substack{n,m=1 \\ m\neq n}}^{N} \overline{\alpha}_n \overline{\alpha}_m \cos\left(2\pi B_c \tau_{n,m} h + \phi_{n,m}\right) \right] . \tag{12}$$

For shortness, (12) can be written as $\bar{\bar{\gamma}}(\mathbf{s}) = G(\mathbf{s}) + V(\mathbf{s})$ where

$$\begin{aligned} G(\mathbf{s}) &= \sum_{n=1}^{N} \overline{\alpha_n^2} \ ; \quad V(\mathbf{s}) = \sum_{\substack{n,m=1 \\ m\neq n}}^{N} \overline{\alpha}_n \overline{\alpha}_m \nu_{n,m} \ ; \\ \nu_{n,m} &= \frac{1}{C} \sum_{h=0}^{C-1} \cos\left(2\pi B_c \tau_{n,m} h + \phi_{n,m}\right) \ . \end{aligned} \tag{13}$$

The term $G(\mathbf{s})$ models the effect of "macroscopic" propagation phenomena, included path loss and signal power absorbed by obstructing objects, which are unaffected by channel switching. Conversely, $V(\mathbf{s})$ accounts for the self-interference among multipath components, which may change by shifting the carrier frequency.

Assuming that $\phi_{n,m}$ takes uniform random values in the interval $[0, 2\pi]$ when varying $\mathbf{s}$, independently of the other variables, we easily realize that

$$\mathrm{m}_{\bar{\bar{\gamma}}} = \mathrm{m}_G \ , \quad \sigma^2_{\bar{\bar{\gamma}}} = \sigma^2_G + \sigma^2_V \tag{14}$$

$$\mathrm{m}_V = 0 \ , \quad \sigma^2_V = \mathrm{E}\left[\sum_{\substack{n,m=1 \\ m\neq n}}^{N} \bar{\alpha}_n^2 \bar{\alpha}_m^2 \nu_{n,m}^2 \right] \tag{15}$$

where m and σ^2 denote mean and variance of the random variable over all possible transceiver positions $\mathbf{s}$ at distance $\|\mathbf{s}\|_2 = d$. We hence see that MCRA can reduce σ^2_V by acting on the coefficients $\nu^2_{n,m}$, which can be expressed as (see [12])

$$\nu^2_{n,m} = \cos(y_{n,m})^2 \, \mathrm{psinc}(B_c \tau_{n,m}, C)^2 \tag{16}$$

where $y_{n,m} = \phi_{n,m} + \pi(C-1) B_c \tau_{n,m}$, while $\mathrm{psinc}(x,n) = \sin(n\pi x)/[n\sin(\pi x)]$ denotes the periodic sinc function.

As known, the squared psinc function has period 1 and its *envelope* is minimized at the center of each period: the larger C, the flatter the envelope around its minimum and, in turn, the lower the energy per period. Therefore, MCRA is most effective when the bandwidth swept by MCRA is large and the inter-cluster delays are widely distributed in the period $1/B_c$. Conversely, the smaller $B_c\tau_{n,m}$, the less effective the MCRA. Since MCRA cannot reduce $\sigma^2_{\bar{\bar{\gamma}}}$ below σ^2_G, as for (14), the larger benefit is obtained when the environment is rather homogeneous (i.e., variance of $\overline{\alpha_n^2}$ is low), and most of the signal power variability is due to self-interference among strong reflections of the signal.

As an example, consider the IEEE 802.15.4 standard that defines $C = 16$ RF channels spaced apart by $B_c = 5$ MHz, centered in the ISM band at 2.4 GHz. The typical delay spread at these frequencies in indoor environments varies from tens to hundreds of nanoseconds [13], [14]. In this case, the MCRA can reduce the energy of the squared psinc function to less than 30% of its initial value, thus effectively reducing σ_V^2.

IV. Experimental results

In this section we present the results of some experiments carried out in different environments. All the experiments have been performed by using TmoteSky sensor nodes [15], which are equipped with the Chipcon wireless transceiver CC2420 implementing the IEEE 802.15.4 standard. The boards have been modified to use an isotropic external antenna rather than the integrated patch antenna, which is strongly anisotropic [16]. A simple communication protocol has been implemented to collect RSS samples over all the 16 RF channels mandated by the IEEE 802.15.4 standard.[1] Data have been collected in four indoor scenarios (Room, Desk, Aisle, Lab) and one Outdoor scenario. In all experiments nodes are in direct visibility (LOS) and placed at the same height. The description of the testbeds and all the collected RSS measurements can be downloaded from the SIGNET group website[2] or contacting the authors.

Some results obtained from Room scenario are reported in the composite Fig. 1. Upper, mid and lower graphs have been obtained from raw RSS data, time-averaged RSS values, and MCRA, respectively. Note that averages are always performed in linear scale and the mean values are converted back in dB scale.

The graphs on the left-hand side show the path loss curve (line) estimated from the corresponding set of RSS values (marks). The parameters $\mathcal{K}$ and η of the path loss model (2) have been estimated from the RSS data using the LS method, with $\delta_0 = 0.6$ m. The error term Ψ^{dB} is then obtained by subtracting the estimated path loss component $D(d)$ from the RSS data. The estimated channel parameters are reported in the caption of each subfigure.

Comparing the three figures we see that time average brings negligible effect which means that, in this scenario, the short-term fading has limited impact on the RSS variability. This result is probably due to the presence of a dominant

[1]We verified experimentally that channel switching is performed in few milliseconds, so that multichannel RSS harvesting between a pair of nodes can be completed in a fraction of second.

[2]http://telecom.dei.unipd.it/download

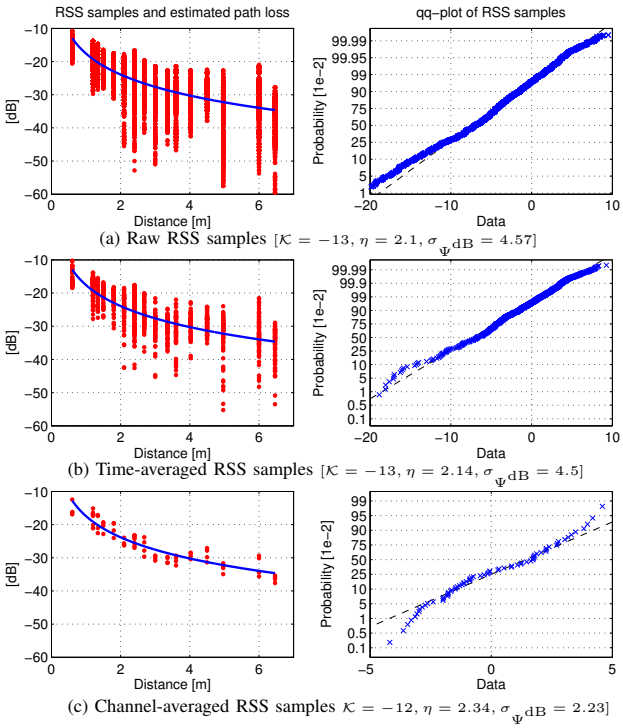

Figure 1: RSS data and channel parameters estimate in Room scenario.

component in the received signal, compatible with a Rician fading model with large Rice factor. Conversely, MCRA yields a significant reduction of $\sigma_{\Psi^{\mathrm{dB}}}$, which drops from about 4.6 down to 2.2, with an improvement of ~ 2.4. Very similar results have been observed in the other scenarios, both indoor and outdoor, not reported here for the sake of conciseness.

On the right-hand side of Fig. 1 we show the quantile-quantile plot (qqplot) of the sample quantiles of Ψ^{dB} versus theoretical quantiles of the distributions that exhibit better fit with the experimental data, namely Extreme Value distribution in case (a) and (b), and normal distribution in case (c). The Extreme Value model for Ψ^{dB} (which corresponds to the Weibull model in linear scale) has been empirically observed in many different experimental campaigns, both in indoor and outdoor environments [4], [17]–[19]. Instead, the normal distribution that is commonly assumed for Ψ^{dB} is actually verified only when RSS are averaged over different channels.

These results are in good agreement with the multi-cluster channel model of Sec. III. Indeed, the empirical distribution of Ψ^{dB} is rather similar to that obtained from the multicluster model (9) when $\{\alpha_n\}$ are modeled as Rician random variables with Rice factor $\mathcal{R} = 30$, and when cluster delays τ_n are uniformly distributed in the interval $[t_0, t_{\max}]$, with $t_{\max} - t_0 \simeq 50$ ns, which is reasonable in indoor environments [11], [13]. The good match between the distributions obtained from empirical data and the multicluster theoretical model confirms the goodness of the model and the effectiveness of the MCRA technique to increase the accuracy of RSS measurements.

Fig. 2 shows the value of $\sigma_{\Psi^{\mathrm{dB}}}$, σ_{ε_r}, and $|\mathrm{m}_{\varepsilon_r}|$ obtained in the different scenarios by averaging the RSS values respectively in time, and over 6 and 16 RF-channels equally

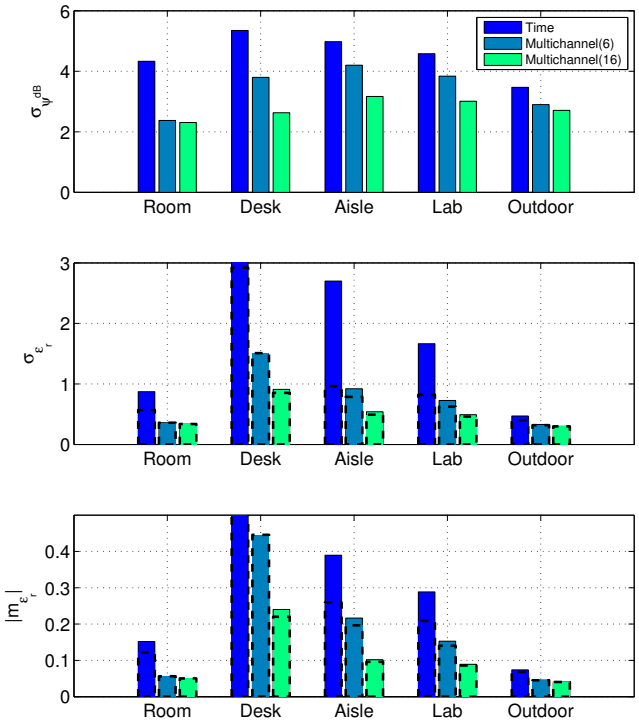

Figure 2: Impact of time and frequency average on $\sigma_{\Psi^{\mathrm{dB}}}$ (upper), σ_{ε_r} (mid), and $|\mathrm{m}_{\varepsilon_r}|$ (lower). Groups of three bars refer to the different scenarios. In each group, the left, central and right bars refer to time-averaged RSS, 6-channel MCRA, and 16-channel MCRA, respectively. Dashed bars in the mid and lower graphs are obtained from (7).

spaced in the 80 MHz of the ISM band. The empirical values of σ_{ε_r} and $|\mathrm{m}_{\varepsilon_r}|$ (solid bars) have been compared with the theoretical values (dashed bars) given by (7) for the corresponding $\sigma = \sigma_{\Psi^{\mathrm{dB}}}/A$. We can observe that MCRA significantly decreases $\sigma_{\Psi^{\mathrm{dB}}}$, thus reducing both σ_{ε_r} and $|\mathrm{m}_{\varepsilon_r}|$ in all scenarios. Furthermore, MCRA performance is almost the same for 6 and 16 RF channels, which confirms that, if $B_c\tau_{n,m}$ is large enough, MCRA can be effective even for small values of C. Finally, we see that empirical and theoretical values of $\mathrm{m}_{\varepsilon_r}$ and σ_{ε_r} are in excellent agreement when MCRA is used, while the empirical error is sometimes larger than the theoretical one for the single-channel RSS case. The reason is that equations (7) assume lognormal distribution of Ψ and ε_r, which is indeed observed only after MCRA.

V. Conclusions

In this letter, we claimed that the accuracy of RSS measurements and RSS-based ranging in common wireless systems can be significantly ameliorated by averaging multiple RSS samples harvested on different RF channels. To sustain this claim, we proposed a theoretical analysis of the effect of MCRA on the variance of the RSS, and a set of experimental results obtained in different scenarios. The study confirms that MCRA is effective in reducing the component of RSS variance due to strong multipath interference, while it does not affect the RSS variations due to path-loss and obstructions. In turn, MCRA can increase the accuracy of RSS-based ranging, provided that the delay spread is large enough.

The price to pay for this gain is the higher complexity of the communication protocol that has to synchronize the nodes to a common channel hopping sequence. However, we noted that most of the performance gain can be attained by collecting RSS samples on just few channels, provided that $B_c\tau_{n,m}$ is large enough. Since channel switching occurs in different time instants, furthermore, MCRA also guarantees time diversity and, hence, short-term fading compensation. Finally, we observe that, given the number of RSS samples, MCRA has basically the same energetic cost of single-channel RSS ranging because channel switching is not an energy consuming operation. In conclusion, MCRA is as a simple but effective strategy to increase the accuracy of RSS measurements and RSS-based ranging in wireless systems.

VI. Acknowledgements

Authors wish to thank Dr. Francesco Zorzi for his contribution in the early stage of this work.

References

[1] X. Li, "RSS-based location estimation with unknown pathloss model," *IEEE Transactions on Wireless Communications*, vol. 5, no. 12, pp. 3626 –3633, december 2006.

[2] S. Hara, D. Zhao, K. Yanagihara, J. Taketsugu, K. Fukui, S. Fukunaga, and K. Kitayama, "Propagation characteristics of IEEE 802.15.4 radio signal and their application for location estimation," in *Proceedings of the IEEE VTC 2005-Spring.*, vol. 1, june 2005, pp. 97–101.

[3] D. Lymberopoulos, Q. Lindsey, and A. Savvides, "An empirical characterization of radio signal strength variability in 3-d ieee 802.15.4 networks using monopole antennas," in *Wireless Sensor Networks*, ser. Lecture Notes in Computer Science, Springer Berlin/Heidelberg, 2006, vol. 3868, pp. 326–341.

[4] A. Bardella, N. Bui, A. Zanella, and M. Zorzi, "An Experimental Study on IEEE 802.15. 4 Multichannel Transmission to Improve RSSI–Based Service Performance," in *Proceedings of the Real-World Wireless Sensor Networks*, pp. 154–161, 2010.

[5] D. Puccinelli and M. Haenggi, "Multipath fading in wireless sensor networks: measurements and interpretation," in *Proceedings of the ACM IWCMC'06*, New York, NY, USA, 2006, pp. 1039–1044.

[6] A. Goldsmith, *Wireless Communications*, New York, NY, USA: Cambridge University Press, 2005.

[7] A. Saleh and R. Valenzuela, "A statistical model for indoor multipath propagation," *IEEE Journal on Selected Areas in Communications*, vol. 5, no. 2, pp. 128 –137, february 1987.

[8] J. o. d. Nielsen, V. Afanassiev, and J. r. Bach Andersen, "A dynamic model of the indoor channel," *Wireless Personal Communications*, vol. 19, pp. 91–120, 2001.

[9] D. Zhang, Y. Liu, X. Guo, M. Gao, and L. Ni, "On distinguishing the multiple radio paths in RSS-based ranging," in *INFOCOM, 2012 Proceedings IEEE*, march 2012, pp. 2201–2209.

[10] W. Lee, "Elements of cellular mobile radio systems," *IEEE Transactions on Vehicular Technology*, vol. 35, no. 2, pp. 48 – 56, may 1986.

[11] H. Hashemi, "The indoor radio propagation channel," *Proceedings of the IEEE*, vol. 81, no. 7, pp. 943–968, July 1993.

[12] M. P. Knapp, "Sines and cosines of angles in arithmetic progression," *Mathematics Magazine*, vol. 82, no. 5, pp. 371–372, 2009.

[13] H. MacLeod, C. Loadman, and Z. Chen, "Experimental studies of the 2.4-HGz ISM wireless indoor channel," in *Proceedings of Communication Networks and Services Research Conference, 2005.*, may 2005, pp. 63–68.

[14] H.-J. Zepernick and T. Wysocki, "Multipath channel parameters for the indoor radio at 2.4 GHz ISM band," in *Proceedings of IEEE Vehicular Technology Conference, 1999*, vol. 1, jul 1999, pp. 190–193 vol.1.

[15] "Tmote sky: Ultra low power IEEE 802.15.4 compliant wireless sensor module," Moteiv. [Online]. Available: http://www.eecs.harvard.edu/~konrad/projects/shimmer/references/tmote-sky-datasheet.pdf

[16] "CC2420: 2.4 GHz IEEE 802.15.4 / ZigBee-ready RF Transceiver," Chipcon Products from Texas Instruments. [Online]. Available: http://http://www.ti.com/lit/ds/swrs041b/swrs041b.pdf

[17] N. Shepherd, “Radio wave loss deviation and shadow loss at 900 MHz,” in *Proceedings of IEEE Vehicular Technology Conference*, vol. 26, march 1976, pp. 63–66.

[18] F. Babich, G. Lombardi, L. Tomasi, and E. Valentinuzzi, “Indoor propagation measurements at DECT frequencies,” in *Proceedings of Electrotechnical Conference*, vol. 3, may 1996, pp. 1355 –1359 vol.3.

[19] G. Tzeremes and C. Christodoulou, “Use of Weibull distribution for describing outdoor multipath fading,” in *Proceedings of IEEE Antennas and Propagation Society International Symposium*, vol. 1, 2002, pp. 232 – 235 vol.1.